

# Bifurcated states of a rotating tokamak plasma in the presence of a static error-field

Richard Fitzpatrick

*Institute for Fusion Studies, Department of Physics, The University of Texas at Austin, Austin, Texas 78712*

(Received 20 January 1998; accepted 1 June 1998)

The bifurcated states of a rotating tokamak plasma in the presence of a static, resonant, error-field are strongly analogous to the bifurcated states of a conventional induction motor. The two plasma states are the “unreconnected” state, in which the plasma rotates and error-field-driven magnetic reconnection is suppressed, and the “fully reconnected” state, in which the plasma rotation at the rational surface is arrested and driven magnetic reconnection proceeds without hindrance. The response regime of a rotating tokamak plasma in the vicinity of the rational surface to a static, resonant, error-field is determined by *three* parameters: the normalized plasma viscosity,  $P$ , the normalized plasma rotation,  $Q_0$ , and the normalized plasma resistivity,  $R$ . There are 11 distinguishable response regimes. The extents of these regimes are calculated in  $P$ - $Q_0$ - $R$  space. In addition, an expression for the critical error-field amplitude required to trigger a bifurcation from the “unreconnected” to the “fully reconnected” state is obtained in each regime. The appropriate response regime for low-density, ohmically heated, tokamak plasmas is found to be the nonlinear *constant- $\psi$*  regime for small tokamaks, and the linear *constant- $\psi$*  regime for large tokamaks. The critical error-field amplitude required to trigger error-field-driven magnetic reconnection in such plasmas is a rapidly decreasing function of machine size, indicating that particular care may be needed to be taken to reduce resonant error-fields in a reactor-sized tokamak. © 1998 American Institute of Physics. [S1070-664X(98)01409-8]

## I. INTRODUCTION

The magnetic field of a tokamak is supposed to be toroidally symmetric. In reality, of course, there is always a slight deviation from pure toroidal symmetry due to the misalignment of field coils, the presence of non-axisymmetric current feeds, etc. It is conventional to describe the field as a superposition of the desired axisymmetric field,  $\mathbf{B}$ , plus an accidentally produced non-axisymmetric “error-field,”  $\delta\mathbf{B}$ . The typical magnitude of the error-field in present day tokamak experiments is  $10^{-4}$  of the axisymmetric toroidal magnetic field strength.

In a large aspect ratio, low- $\beta$ ,<sup>1</sup> circular flux-surface tokamak<sup>2</sup> the error-field can be resolved into Fourier harmonics expressed in terms of the toroidal ( $\phi$ ) and poloidal ( $\theta$ ) angles around the device. The Fourier harmonics of the error-field fall into two classes: “resonant” and “nonresonant.” For a resonant harmonic there exists a “rational flux surface” inside the plasma for which  $\mathbf{k} \cdot \mathbf{B} = 0$ , where  $\mathbf{k}$  is the wave vector associated with the harmonic. For a nonresonant harmonic there is no corresponding rational surface inside the plasma. Nonresonant harmonics of the error-field give rise to a non-axisymmetric displacement of plasma flux surfaces, but generally have no discernible effect on the energy confinement properties of the plasma. Resonant harmonics also give rise to a non-axisymmetric displacement of flux surfaces, but, in addition, they cause “reconnection” of magnetic field lines in the vicinity of the associated rational surfaces. This effect is of some concern to fusion scientists, since when field lines reconnect they give rise to the formation of “magnetic islands,” and magnetic islands are known

to degrade the energy confinement properties of tokamak plasmas.<sup>3</sup> In fact, if the islands become too large, or too numerous, then they can trigger a catastrophic loss of confinement known as a “disruption.”<sup>4</sup>

One would naively expect a tokamak plasma subject to an error-field (as all tokamak plasmas are) to be filled with magnetic islands induced by the various resonant harmonics of the field. Fortunately, this is not generally the case. Tokamak plasmas naturally *rotate*, due to plasma diamagnetism, at a rate which is far larger than the rate at which magnetic reconnection typically proceeds. Under these circumstances, the magnetic islands driven by the resonant components of the error-field are “suppressed,” and the energy confinement properties of the plasma remain unimpaired. However, if any of the resonant Fourier harmonics of the error-field exceed a certain threshold value, then they can trigger a *bifurcation* of the plasma state, in which the plasma rotation at the associated rational surface is halted, and a magnetic island chain subsequently forms. Naturally, there is a degradation of the energy confinement properties of the plasma associated with such a bifurcation.

At present, there are many dissimilar, and apparently contradictory, theories of the response of a rotating tokamak plasma to a static, resonant error-field. The three leading theories are the linear-layer-based approach of Fitzpatrick,<sup>5,6</sup> the Sweet–Parker-based approach of Bhattacharjee and co-workers,<sup>7,8</sup> and the Alfvén resonance based approach of Jensen and co-workers.<sup>9</sup> The main aim of this paper is to demonstrate that these theories are not contradictory, but merely correspond to different limits of a more general

theory which allows for either a *linear* or a *nonlinear* response of the plasma in the vicinity of the rational surface to the applied error-field.

This paper is organized as follows. The problem under investigation is formally set out in Sec. II. In Sec. III the linear response theory of Fitzpatrick is reviewed. The new nonlinear response theory is described in Sec. IV. The relevance of this new theory to tokamak experiments is examined in Sec. V. Finally, the paper is summarized and conclusions are drawn in Sec. VI.

## II. PRELIMINARY ANALYSIS

### A. Introduction

The main aim of this section is to formally set out the problem under investigation in this paper.

### B. The plasma equilibrium

Consider a large-aspect-ratio, low- $\beta$  tokamak plasma<sup>2</sup> whose magnetic flux surfaces map out (almost) concentric circles in the poloidal plane. Such a plasma is well approximated as a periodic cylinder. Suppose that the minor radius of the plasma is  $a$ . Standard cylindrical polar coordinates  $(r, \theta, z)$  are adopted. The system is assumed to be periodic in the  $z$  direction, with periodicity length  $2\pi R_0$ , where  $R_0$  is the simulated major radius of the plasma. It is convenient to define a simulated toroidal angle  $\phi = z/R_0$ .

The equilibrium magnetic field is written  $\mathbf{B} = [0, B_\theta(r), B_\phi]$ . The associated equilibrium plasma current takes the form  $\mathbf{j} = [0, 0, j_\phi(r)]$ , where

$$\mu_0 j_\phi(r) = \frac{1}{r} \frac{d(rB_\theta)}{dr}. \quad (1)$$

The ‘‘safety factor’’

$$q(r) = \frac{rB_\phi}{R_0 B_\theta} \quad (2)$$

parametrizes the helical pitch of the field lines. In a conventional tokamak plasma  $q(r)$  is  $O(1)$ , and is a monotonically increasing function of the flux-surface radius,  $r$ .

### C. The plasma response

Consider the response of the plasma to a static, helical error-field with  $m$  periods in the poloidal direction and  $n$  periods in the toroidal direction. It is convenient to represent the perturbed magnetic field and the perturbed plasma current in terms of a flux function,  $\psi$ :

$$\delta\mathbf{B} = \nabla\psi \wedge \hat{\mathbf{z}}, \quad (3a)$$

$$\mu_0 \delta\mathbf{j} = \nabla \wedge \delta\mathbf{B} = -\nabla^2 \psi \hat{\mathbf{z}}. \quad (3b)$$

Of course,

$$\psi(r, \theta, \phi, t) = \psi(r) \exp[i(m\theta - n\phi)]. \quad (4)$$

This representation is valid provided that

$$\frac{m}{n} \gg \frac{a}{R_0}. \quad (5)$$

The response of the plasma to the applied error-field is governed by the equations of *marginally stable, ideal magnetohydrodynamics (ideal MHD)* everywhere apart from a relatively narrow region in the vicinity of the ‘‘rational surface,’’ radius  $r_s$ , where  $q(r_s) = m/n$ .

It is convenient to parametrize the strength of the error-field in terms of the ‘‘vacuum flux,’’  $\Psi_v$ , which is defined to be the value of  $\psi(r)$  at radius  $r_s$  in the presence of the error-field but in the absence of plasma. Likewise, the response of the plasma in the vicinity of the rational surface to the error-field is parametrized in terms of the ‘‘reconnected magnetic flux,’’  $\Psi_s$ , which is the actual value of  $\psi(r)$  at radius  $r_s$  in the presence of both the error-field and plasma. The relationship between  $\Psi_s$  and  $\Psi_v$  is<sup>6</sup>

$$\Psi_s = \frac{2m}{-\Delta' + \Delta(\omega)} \Psi_v. \quad (6)$$

Here,

$$\Delta' = \left[ r \frac{d\psi_{\text{plasma}}}{dr} \right]_{r_{s-}}^{r_{s+}} \quad (7)$$

is the conventional ‘‘tearing stability index,’’ and  $\psi_{\text{plasma}}(r)$  is a solution to the ideal MHD equations which satisfies physical boundary conditions at  $r=0$  and  $r \rightarrow \infty$  (in the absence of an error-field), and is normalized to unity at the rational surface. According to conventional tearing mode theory,<sup>10</sup> if  $\Delta' > 0$ , then the magnetic field spontaneously reconnects at the rational surface to form a magnetic island. Note that such an island is locked into the frame of the plasma at the rational surface, and, therefore, *rotates* in the laboratory frame. The oscillation frequency of the magnetic field associated with a spontaneously created magnetic island is

$$\omega_0 = m\Omega_{\theta_0}(r_s) - n\Omega_{\phi_0}(r_s), \quad (8)$$

where  $\Omega_{\theta_0}(r)$  and  $\Omega_{\phi_0}(r)$  are the poloidal and toroidal angular velocities of the plasma, respectively, in the absence of an error-field. In the following, it is assumed that  $\Delta' < 0$ , so that the plasma is *intrinsically tearing stable*. In this situation, any magnetic reconnection which takes place inside the plasma is due solely to the externally applied error-field. Such reconnection is known as ‘‘forced reconnection.’’

The complex quantity  $\Delta(\omega)$ , appearing in Eq. (6), parametrizes the response of the nonideal plasma in the vicinity of the rational surface to the applied error-field. Here, the ‘‘slip frequency,’’  $\omega$ , is minus the oscillation frequency of the error-field, as seen in the rotating frame of the plasma at the rational surface. Thus,

$$\omega = m\Omega_{\theta}(r_s) - n\Omega_{\phi}(r_s), \quad (9)$$

where  $\Omega_{\theta}(r)$  and  $\Omega_{\phi}(r)$  are the poloidal and toroidal angular velocities of the plasma, respectively, in the presence of the error-field.

### D. Toroidal torque balance

It is easily demonstrated that *zero* net torque can be exerted on flux surfaces located in a region of the plasma which is governed by the equations of ideal MHD.<sup>6</sup> Thus, the elec-

tromagnetic torque exerted on the plasma by the error-field develops in the immediate vicinity of the rational surface, where ideal MHD breaks down. The net *toroidal* electromagnetic torque exerted in the vicinity of the rational surface by the error-field is written<sup>6</sup>

$$\begin{aligned} \delta T_{\phi \text{ EM}} &= \frac{2\pi^2 n R_0}{\mu_0} \text{Im}(\Delta) |\Psi_s|^2 \\ &= \frac{8\pi^2 n m^2 R_0}{\mu_0} \frac{\text{Im}(\Delta)}{|(-\Delta') + \Delta|^2} |\Psi_v|^2, \end{aligned} \quad (10)$$

where use has been made of Eq. (6).

Of course, the error-field also exerts a *poloidal* torque on the plasma in the vicinity of the rational surface. However, it turns out that tokamak plasmas possess strong parallel (to the magnetic field) viscosity which opposes the plasma compression associated with poloidal rotation.<sup>11</sup> In fact, in conventional tokamak plasmas this viscosity is sufficiently large to prevent any error-field-induced change in the poloidal rotation. Thus, in practice, the plasma does not respond to the poloidal component of the electromagnetic torque exerted in the vicinity of the rational surface by the error-field.<sup>6</sup> On the other hand, the plasma is free to respond to the toroidal component of the electromagnetic torque by changing its toroidal rotation.

Suppose that the change in the toroidal angular velocity of the plasma induced by the error-field is  $\Delta\Omega_\phi(r)$ . It is assumed that perpendicular viscosity acts to relax the rotation profile back to that of the unperturbed plasma (i.e., it tries to make  $\Delta\Omega_\phi$  zero). The boundary condition at the edge of the plasma,  $r = a$ , is

$$\Delta\Omega_\phi(a) = 0. \quad (11)$$

In other words, the plasma rotation is clamped at the edge, and is not substantially modified by the error-field. It is easy to demonstrate theoretically that this is a reasonable assumption.<sup>6</sup> Perpendicular viscosity gives rise to a localized viscous torque, acting in the vicinity of the rational surface, which *opposes* the error-field-induced change in the plasma rotation. In a *steady state* this viscous restoring torque takes the form<sup>6</sup>

$$\delta T_{\phi \text{ VS}} = \frac{-4\pi^2 R_0^3 \Delta\Omega_{\phi s}}{\int_r^a dr/r\mu}, \quad (12)$$

where  $\Delta\Omega_{\phi s} \equiv \Delta\Omega_\phi(r_s)$  is the change in the plasma toroidal angular velocity at the rational surface, and  $\mu(r)$  is the perpendicular (to the magnetic field) viscosity of the plasma.

The error-field-induced change in the toroidal rotation of the plasma gives rise to a modification of the ‘‘slip frequency’’ (i.e., minus the oscillation frequency of the error-field seen in the rotating frame of the plasma at the rational surface). According to Eqs. (8) and (9) (assuming that poloidal flow is strongly damped),

$$\omega = \omega_0 - n\Delta\Omega_{\phi s}, \quad (13)$$

where  $\omega_0$  is the oscillation frequency of a naturally unstable (i.e.,  $\Delta' > 0$ )  $m/n$  tearing mode in the unperturbed plasma. This frequency is termed the ‘‘natural frequency.’’

In a *steady state*, the electromagnetic and viscous torques acting on the plasma in the vicinity of the rational surface must balance. Thus,

$$\delta T_{\phi \text{ EM}} + \delta T_{\phi \text{ VS}} = 0. \quad (14)$$

It follows from Eqs. (10), (12), and (13) that the toroidal torque balance equation can be written<sup>6</sup>

$$\frac{2n^2 m^2 (\int_r^a dr/r\mu)}{\mu_0 R_0^2} \frac{\text{Im}(\Delta)}{|(-\Delta') + \Delta|^2} |\Psi_v|^2 = \omega_0 - \omega. \quad (15)$$

### E. Bifurcation analysis

For all of the plasma response functions,  $\Delta(\omega)$ , considered in this paper, the above torque balance equation possesses *two* separate branches of solutions.<sup>6</sup> On the ‘‘unreconnected’’ branch, which is characterized by  $|\Delta| \gg (-\Delta')$ , the plasma in the vicinity of the rational surface rotates sufficiently rapidly (i.e.,  $\omega \sim \omega_0$ ) to effectively suppress error-field-driven magnetic reconnection (i.e.,  $|\Psi_s| \ll |\Psi_v|$ ). On the ‘‘fully reconnected’’ branch of solutions, which is characterized by  $|\Delta| \sim (-\Delta')$ , the plasma rotation at the rational surface is arrested (i.e.,  $\omega \ll \omega_0$ ), and error-field-driven reconnection proceeds without hindrance (i.e.,  $|\Psi_s| \sim |\Psi_v|$ ). Bifurcations occur between these two branches of solutions as the strength of the error-field (or the intrinsic plasma rotation) is *very gradually* increased or decreased. There is a critical error-field amplitude which, when exceeded, triggers a ‘‘downward’’ bifurcation: i.e., from the ‘‘unreconnected’’ branch to the ‘‘fully reconnected’’ branch. Likewise, there is a *significantly smaller* critical error-field amplitude below which an ‘‘upward’’ bifurcation (i.e., from the ‘‘fully reconnected’’ branch to the ‘‘unreconnected’’ branch) is triggered.

Note that the important ‘‘downward’’ bifurcation is governed by a simplified version of Eq. (15) [obtained by taking the limit  $|\Delta| \gg (-\Delta')$ ]:

$$-\frac{2n^2 m^2 (\int_r^a dr/r\mu)}{\mu_0 R_0^2} \text{Im} \left[ \frac{1}{\Delta(\omega)} \right] |\Psi_v|^2 = \omega_0 - \omega. \quad (16)$$

It is interesting to note that the bifurcated states of a rotating tokamak plasma in the presence of a static error-field are very reminiscent of the bifurcated states of a conventional induction motor.<sup>12</sup>

## III. LINEAR RESPONSE THEORY

### A. Introduction

The main aims of this section are to review the linear response theory of Fitzpatrick,<sup>5,6</sup> and to introduce the scheme adopted in this paper for classifying the plasma response to the applied error-field.

### B. Linear versus nonlinear response theory

It is legitimate to calculate the plasma response using linear analysis if the linear layer width at the rational surface is *larger* than the width of the magnetic island chain driven by the error-field. This is not likely to be the case on the ‘‘fully reconnected’’ branch of solutions. However, on the

“unreconnected” branch it is possible that the suppression of error-field-driven magnetic reconnection due to plasma rotation is sufficiently strong to keep the driven island width *below* the linear layer width. In fact, it can easily be demonstrated that this is the case provided that the plasma conductivity (which increases strongly with increasing plasma temperature) is sufficiently high (see Sec. IV). Thus, since linear analysis is only appropriate to the “unreconnected” branch of solutions, this section only considers the “downward” bifurcation (because this bifurcation depends solely on the “unreconnected” branch of solutions). A discussion of the “upward” bifurcation is postponed until Sec. IV, which deals with nonlinear response theory.

**C. The layer equations**

The linearized equations of nonideal MHD for a single-fluid, zero- $\beta$ , incompressible plasma reduce to

$$\frac{d^2\psi}{dx^2} = i\omega\tau_R(\psi - x\phi), \tag{17a}$$

$$x \frac{d^2\psi}{dx^2} = (\omega\tau_H)^2 \frac{d^2\phi}{dx^2} + i \frac{\omega\tau_H^2}{\tau_V} \frac{d^4\phi}{dx^4}, \tag{17b}$$

in the vicinity of the rational surface.<sup>13</sup> Here,  $\phi = -sB_\theta(r_s)\xi$  is the normalized radial plasma displacement,  $\xi$  is the actual radial plasma displacement, and  $x = (r - r_s)/r_s$ . Furthermore,

$$s = \left( \frac{r}{q} \frac{dq}{dr} \right)_{r_s}, \tag{18a}$$

$$\tau_H = \frac{R_0}{B_\phi} \frac{\sqrt{\mu_0\rho(r_s)}}{ns}, \tag{18b}$$

$$\tau_R = \mu_0 r_s^2 \sigma(r_s), \tag{18c}$$

$$\tau_V = \frac{r_s^2 \rho(r_s)}{\mu(r_s)} \tag{18d}$$

are the magnetic shear, the hydromagnetic time scale, the resistive diffusion time scale, and the viscous diffusion time scale, respectively, all evaluated at the rational surface. In the above,  $\rho(r)$ ,  $\sigma(r)$ , and  $\mu(r)$  are the plasma mass density, parallel (to the magnetic field) electrical conductivity, and perpendicular resistivity, respectively.

Equations (17) possess a trivial solution ( $\phi = \phi_0$ ,  $\psi = x\phi_0$ , where  $\phi_0$  is independent of  $x$ ), and a nontrivial solution for which  $\psi(-x) = \psi(x)$  and  $\phi(-x) = -\phi(x)$ . The asymptotic behavior of the nontrivial solution at the edge of the layer is

$$\psi(x) \rightarrow \left( \frac{\Delta}{2} |x| + 1 \right) \Psi_s, \tag{19a}$$

$$\phi(x) \rightarrow \frac{\psi}{x}, \tag{19b}$$

where the plasma response function,  $\Delta(\omega)$ , is a complex quantity which can only be determined by solving Eqs. (17). The constant parameter  $\Psi_s$  is identical to the parameter  $\Psi_s$

introduced in Sec. II. Note, however, that this parameter can only be interpreted as the “reconnected magnetic flux” in a constant- $\psi$  regime.

**D. The normalization scheme**

In this paper, the critical error-field amplitude needed to trigger a “downward” bifurcation of the plasma state is calculated for many different response regimes of the plasma. It is convenient to adopt a uniform normalization scheme which easily allows one to compare and contrast the various different expressions for the critical amplitude. This normalization scheme is described below.

The error-field amplitude is measured in terms of the radial displacement,  $\xi_s$ , at the rational surface, calculated assuming that the plasma response to the error-field is *ideal*. This displacement is related to the “vacuum flux,”  $\Psi_v$ , via

$$\xi_s = \frac{2m|\Psi_v|}{sB_\theta(r_s)}. \tag{20}$$

The normalized “slip frequency” is written

$$Q = \tau_H^{2/3} \tau_R^{1/3} \omega. \tag{21}$$

Likewise, the normalized “natural frequency” of the plasma takes the form

$$Q_0 = \tau_H^{2/3} \tau_R^{1/3} \omega_0. \tag{22}$$

The plasma viscosity is parametrized by

$$P = \frac{\tau_R}{\tau_V}. \tag{23}$$

Note that the plasma becomes more viscous as  $P$  increases. Finally, the plasma electrical resistivity is parametrized by

$$R = \kappa^{1/5} \frac{\tau_H^{1/15}}{\tau_R^{1/30} \tau_V^{1/30}}, \tag{24}$$

where

$$\kappa = \left[ \frac{B_\phi}{B_\theta(r_s)} \right]^2 \bigg/ \int_{r_s}^a \frac{\mu(r_s) dr}{\mu(r) r}. \tag{25}$$

Note that the plasma becomes more resistive as  $R$  increases. It is demonstrated in Sec. IV that linear response theory is valid in the low resistivity limit,  $R \ll 1$ .

It is convenient to normalize all widths to the linear layer width

$$\delta_{VR} = \frac{\tau_H^{1/3}}{\tau_R^{1/6} \tau_V^{1/6}} r_s \tag{26}$$

obtained in the *visco-resistive* regime (see later). Thus, the normalized ideal plasma displacement, the normalized plasma response function, and the normalized linear layer width are written

$$\hat{\xi}_s = \frac{\xi_s}{\delta_{VR}}, \tag{27a}$$

$$\hat{\Delta} = \Delta \frac{\delta_{VR}}{r_s}, \tag{27b}$$

$$\hat{\delta}_s = \frac{\delta_s}{\delta_{VR}}, \tag{27c}$$

respectively.

### E. Linear layer physics

The linearized layer equations (17) can be solved, subject to the boundary conditions (19), to obtain the complex quantity  $\hat{\Delta}$  which fully describes the response of the layer to the error-field.<sup>13</sup> It turns out that there are *four* distinct linear response regimes. In the *visco-resistive* regime, plasma inertia is negligible inside the layer, and

$$\hat{\Delta} = -2.104 e^{-i\pi/2} P^{1/3} Q, \tag{28a}$$

$$\hat{\delta}_s \sim 1. \tag{28b}$$

In the *resistive-inertial* regime, plasma viscosity is negligible inside the layer, and

$$\hat{\Delta} = -2.124 e^{-i3\pi/8} P^{1/6} Q^{5/4}, \tag{29a}$$

$$\hat{\delta}_s \sim P^{-1/6} Q^{1/4}. \tag{29b}$$

In the *visco-inertial* regime, plasma resistivity is negligible inside the layer, and

$$\hat{\Delta} = -4.647 e^{-i\pi/8} P^{-1/12} Q^{-1/4}, \tag{30a}$$

$$\hat{\delta}_s \sim P^{1/12} Q^{1/4}. \tag{30b}$$

Finally, in the *inertial* regime, both plasma resistivity and plasma viscosity are negligible inside the layer, and

$$\hat{\Delta} = -3.142 e^{-i\pi/2} P^{1/6} Q^{-1}, \tag{31a}$$

$$\hat{\delta}_s \sim P^{-1/6} Q. \tag{31b}$$

In the above formulas it is assumed that  $Q > 0$ , for the sake of definiteness. The region of validity, in  $P$ - $Q$  space, of the four response regimes described above is sketched in Fig. 1.

The *constant- $\psi$*  approximation<sup>10</sup> holds whenever the perturbed magnetic flux  $\psi(r)$  is approximately constant across the layer. In this limit, the quantity  $\Psi_s$ , defined in Eqs. (19), can be interpreted as the ‘‘reconnected magnetic flux.’’ The constant- $\psi$  approximation is valid provided that  $\Delta \delta_s / r_s \ll 1$ , or

$$\hat{\Delta} \hat{\delta}_s \ll 1. \tag{32}$$

It follows from Eqs. (28)–(31) that for high-viscosity plasmas (i.e.,  $P \gg 1$ )

$$\hat{\Delta} \hat{\delta}_s \sim P^{1/3} Q \quad \text{for } Q \ll P^{-1/3}, \tag{33a}$$

$$\hat{\Delta} \hat{\delta}_s \sim 1 \quad \text{for } Q \gg P^{-1/3}. \tag{33b}$$

Likewise, for low-viscosity plasmas (i.e.,  $P \ll 1$ ),

$$\hat{\Delta} \hat{\delta}_s \sim P^{1/3} Q \quad \text{for } Q \ll P^{2/3}, \tag{34a}$$

$$\hat{\Delta} \hat{\delta}_s \sim Q^{3/2} \quad \text{for } P^{2/3} \ll Q \ll 1, \tag{34b}$$

$$\hat{\Delta} \hat{\delta}_s \sim 1 \quad \text{for } Q \gg 1. \tag{34c}$$

Clearly, the constant- $\psi$  approximation holds in the *visco-resistive* and *resistive-inertial* regimes, and breaks down in

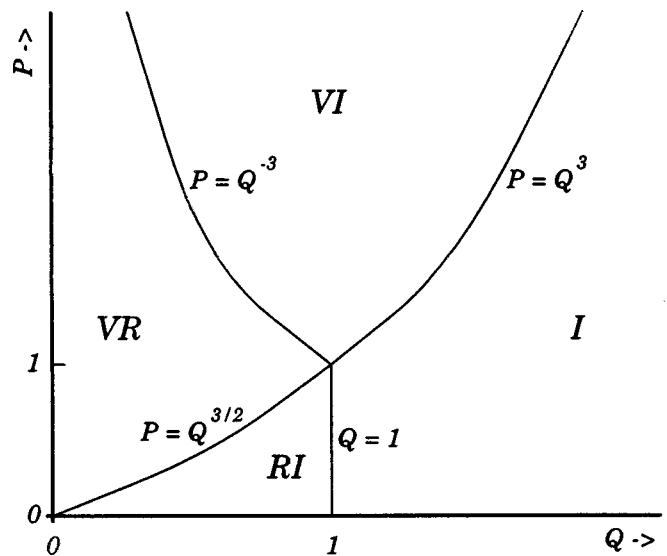


FIG. 1. A schematic diagram showing the extent of the four linear response regimes in normalized viscosity,  $P$ , versus normalized ‘‘slip frequency,’’  $Q$ , space. The four regimes are the *visco-resistive* regime (VR), the *resistive-inertial* regime (RI), the *visco-inertial* regime (VI), and the *inertial* regime (I).

the *visco-inertial* and *inertial* regimes (see Fig. 1). At fixed plasma viscosity (i.e., fixed  $P$ ), the dimensionless parameter  $\hat{\Delta} \hat{\delta}_s$  increases monotonically with increasing ‘‘slip frequency’’ (i.e., with increasing  $Q$ ), until a critical ‘‘slip frequency’’ is reached above which the constant- $\psi$  approximation breaks down. Beyond this critical frequency, the dimensionless parameter  $\hat{\Delta} \hat{\delta}_s$  ceases to increase with  $Q$ , and, instead, saturates at a constant value which is of order unity.

In both nonconstant- $\psi$  regimes, plasma resistivity is negligible in the nonideal layer centered on the rational surface. It follows from Eq. (17a) that  $\psi \approx x \phi$  in all nonconstant- $\psi$  layers. In other words,  $\psi$  is zero at the center of a nonconstant- $\psi$  layer (i.e.,  $x = 0$ ), despite the fact that  $\psi$  at the edge of the layer (i.e.,  $\Psi_s$ ) is nonzero. It is easily demonstrated that in the *inertial* regime the layer actually consists of *two* separate viscous layers of normalized width  $\hat{\delta}_v = P^{1/12} Q^{1/4}$ , centered on the Alfvén resonances [i.e., the two flux surfaces which satisfy  $x^2 = (\omega \tau_H)^2$ ].<sup>14,15</sup> The normalized layer width in the *inertial* regime,  $\hat{\delta}_s = P^{-1/6} Q$ , is simply the normalized radial separation of the Alfvén resonances. In the *visco-inertial* regime, the two Alfvén resonances are sufficiently close together that their viscous layers overlap. Thus, the normalized layer width in the *visco-inertial* regime,  $\hat{\delta}_s = P^{1/12} Q^{1/4}$ , is the normalized width of the common viscous layer surrounding the two Alfvén resonances. It is easily shown that, in marked contrast to the two constant- $\psi$  regimes, there is essentially *zero* magnetic reconnection in the two nonconstant- $\psi$  regimes (i.e., no error-field-driven magnetic islands are formed in the two nonconstant- $\psi$  regimes).<sup>9</sup>

### F. The normalized torque balance equation

The normalized torque balance equation [i.e., the normalized version of Eq. (16)] can be written

$$\delta \hat{T}_{\phi EM} = \delta \hat{T}_{\phi VS}, \tag{35}$$

where the normalized viscous torque takes the form

$$\delta \hat{T}_{\phi \text{ VS}} = Q_0 - Q, \tag{36}$$

and the normalized electromagnetic torque is written

$$\delta \hat{T}_{\phi \text{ EM}} = - \frac{\text{Im}(\hat{\Delta}^{-1})}{2P^{1/3}R^5} \hat{\xi}_s^2. \tag{37}$$

The electromagnetic torque takes the form

$$\delta \hat{T}_{\phi \text{ EM}} = 0.2376 P^{-2/3} Q^{-1} R^{-5} \hat{\xi}_s^2 \tag{38}$$

in the *visco-resistive* regime,

$$\delta \hat{T}_{\phi \text{ EM}} = 0.2175 P^{-1/2} Q^{-5/4} R^{-5} \hat{\xi}_s^2 \tag{39}$$

in the *resistive-inertial* regime,

$$\delta \hat{T}_{\phi \text{ EM}} = 0.0412 P^{-1/4} Q^{1/4} R^{-5} \hat{\xi}_s^2 \tag{40}$$

in the *visco-inertial* regime, and

$$\delta \hat{T}_{\phi \text{ EM}} = 0.1591 P^{-1/2} QR^{-5} \hat{\xi}_s^2 \tag{41}$$

in the *inertial* regime.

In general, the electromagnetic torque (on the ‘‘unreconnected’’ branch of solutions) decreases monotonically with increasing  $Q$  in the constant- $\psi$  regimes, and increases monotonically with increasing  $Q$  in the nonconstant- $\psi$  regimes.<sup>5</sup> The normalized torque attains its minimum value at the boundary between the constant- $\psi$  and nonconstant- $\psi$  regimes.

### G. Bifurcation analysis

The normalized ‘‘slip frequency,’’  $Q$ , is determined from the crossing point of the normalized viscous torque curve (36) and the normalized electromagnetic torque curve specified in Eqs. (38)–(41). As the normalized plasma displacement,  $\hat{\xi}_s$ , is *very gradually* increased from a small value, the crossing point, which initially occurs at  $Q = Q_0$ , occurs at ever smaller values of  $Q$  (i.e., the plasma rotation at the rational surface slows down). Furthermore, it is easily demonstrated that the two curves cease to cross above some critical value of the normalized plasma displacement,  $\hat{\xi}_s = \hat{\xi}_c$ . In fact, as this critical value is exceeded the ‘‘unreconnected’’ branch of solutions ceases to exist, and the plasma makes a ‘‘downward’’ bifurcation to the ‘‘fully reconnected’’ branch of solutions.

In the *visco-resistive* regime, the critical value of  $Q$  at which the ‘‘downward’’ bifurcation takes place is  $Q_0/2$  (i.e., the bifurcation takes place when the plasma rotation at the rational surface has been reduced to one half of its value in the absence of an error-field). The critical value of  $\hat{\xi}_s$  needed to trigger such a bifurcation is

$$\hat{\xi}_c = 1.026 P^{1/3} Q_0 R^{5/2}. \tag{42}$$

In the *resistive-inertial* regime, the critical value of  $Q$  at which the ‘‘downward’’ bifurcation takes place is  $(5/9)Q_0$ . The critical value of  $\hat{\xi}_s$  needed to trigger such a bifurcation is

$$\hat{\xi}_c = 0.990 P^{1/4} Q_0^{9/8} R^{5/2}. \tag{43}$$

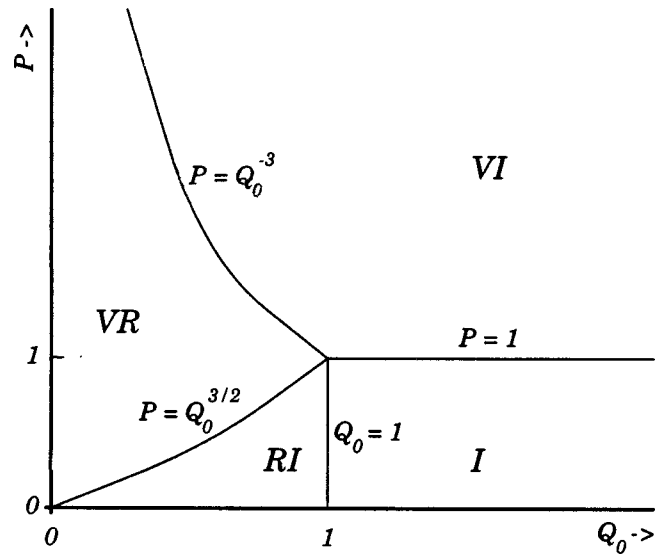


FIG. 2. A schematic diagram showing the extents of the four linear ‘‘downward’’ bifurcation regimes plotted in normalized plasma viscosity,  $P$ , versus normalized plasma rotation  $Q_0$ , space. The four regimes are the *visco-resistive* regime (VR), the *resistive-inertial* regime (RI), the *visco-inertial* regime (VI), and the *inertial* regime (I).

In the two nonconstant- $\psi$  regimes, the critical value of  $Q$  at which the ‘‘downward’’ bifurcation takes place corresponds to that at which the electromagnetic torque attains its minimum value.<sup>5</sup> In the high-viscosity limit,  $P \gg 1$ , the bifurcation takes place when  $Q \approx P^{-1/3}$ , and

$$\hat{\xi}_c \approx P^{1/6} Q_0^{1/2} R^{5/2}. \tag{44}$$

Likewise, in the low-viscosity limit,  $P \ll 1$ , the bifurcation takes place when  $Q \approx 1$ , and

$$\hat{\xi}_c \approx P^{1/4} Q_0^{1/2} R^{5/2}. \tag{45}$$

Figure 2 shows the extent of the four linear ‘‘downward’’ bifurcation regimes in normalized plasma viscosity,  $P$ , versus normalized ‘‘natural frequency,’’  $Q_0$ , space. Each regime is named for the plasma response regime which holds at the point of bifurcation. Thus, in the *visco-resistive* regime,  $\hat{\xi}_c$  is given by Eq. (42); in the *resistive-inertial* regime,  $\hat{\xi}_c$  is given by Eq. (43); in the *visco-inertial* regime,  $\hat{\xi}_c$  is given by Eq. (44); and in the *inertial* regime,  $\hat{\xi}_c$  is given by Eq. (45).

## IV. NONLINEAR RESPONSE THEORY

### A. Introduction

In Sec. III the critical error-field amplitude ( $\hat{\xi}_c$ ) required to trigger a ‘‘downward’’ bifurcation of the plasma state is evaluated in plasma viscosity ( $P$ ) versus plasma rotation frequency ( $Q_0$ ) space, in the limit of low plasma resistivity: i.e.,  $R \ll 1$  (see Fig. 2). The aim of this section is to extend the previous analysis to allow for high plasma resistivity: i.e.,  $R \gg 1$ . This entails calculating the *nonlinear* response of a rotating tokamak plasma in the vicinity of the rational surface to a static, resonant, error-field (i.e., the response when the width of the magnetic island chain driven by the error-field exceeds the linear layer width).

### B. The Rutherford regime

The nonlinear concomitant of the two linear constant- $\psi$  regimes discussed in Sec. III is the well-known *Rutherford regime*.<sup>16,17</sup> In this regime, the constant- $\psi$  approximation remains valid, so that  $\psi(x, \theta, \phi, t) \approx \Psi_s \cos \zeta$  in the vicinity of the rational surface, where  $\Psi_s$  is the ‘‘reconnected magnetic flux,’’ and  $\zeta = m\theta - n\phi - \int^t \omega dt$  is the helical angle. When this expression for the perturbed magnetic flux,  $\psi$ , is superposed on the equilibrium magnetic flux, field-line tracing in the vicinity of the rational surface yields a magnetic island chain, centered on the rational surface, whose maximum width is given by

$$W = 4 \left( \frac{|\Psi_s|}{sr_s B_\theta(r_s)} \right)^{1/2} r_s. \tag{46}$$

The nonlinear evolution equation for the width,  $W$ , of the driven island chain at the rational surface takes the form<sup>5,6,16,17</sup>

$$0.8227 \tau_R \frac{d}{dt} \left( \frac{W}{r_s} \right) = \Delta' + 2m \left( \frac{W_v}{W} \right)^2 \cos \varphi \equiv \text{Re}(\Delta). \tag{47}$$

Here,  $W_v$  is the width of the ‘‘vacuum island’’ chain, which is obtained by superposing the vacuum error-field on the unperturbed plasma equilibrium. It is easily demonstrated that

$$W_v = 4 \left( \frac{|\Psi_v|}{sr_s B_\theta(r_s)} \right)^{1/2} r_s. \tag{48}$$

The phase angle  $\varphi(t)$  is the instantaneous difference in helical angle between the  $O$ -points of the plasma and vacuum island chains at the rational surface.

Note that in the nonlinear regime the plasma in the vicinity of the rational surface is required to *corotate* with the magnetic island, since plasma is trapped inside the magnetic separatrix, whereas in the linear regime the plasma at the rational surface is able to flow with respect to the magnetic perturbation.<sup>5,6</sup> Thus, in the nonlinear regime there is a ‘‘no slip’’ condition which relates the instantaneous rotation frequency,  $\omega(t)$ , of the magnetic island chain to the plasma rotation frequency at the rational surface [see Eq. (13)]:

$$\omega \equiv \frac{d\varphi}{dt} = \omega_0 - n \Delta \Omega_{\phi s}. \tag{49}$$

Here, it is assumed that plasma flow in the poloidal direction is strongly damped.

On the ‘‘unreconnected’’ branch of solutions  $|\Delta| \gg (-\Delta')$ , so the first term on the right-hand side of Eq. (47) is negligible. Furthermore, it is reasonable to assume that the island rotation is essentially uniform (i.e.,  $\omega$  is constant in time). This assumption is justified later on. In this limit, therefore, the island evolution equation (47) can be integrated to give

$$W(t) \approx W_0 |\sin \omega t|^{1/3}, \tag{50}$$

where

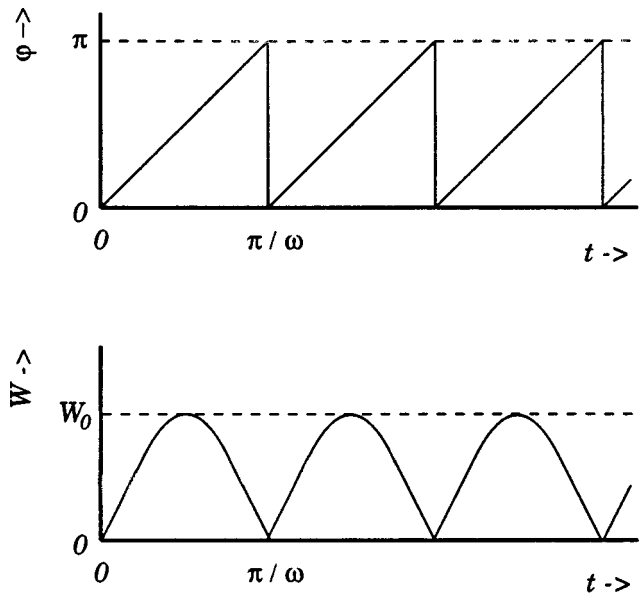


FIG. 3. A schematic diagram showing the time variation of the phase,  $\varphi$  (relative to the error-field), and width,  $W$ , of the magnetic island chain driven by a static error-field in a uniformly rotating plasma.

$$W_0 = 1.939 m^{1/3} \left( \frac{W_v^2 / r_s^2}{\omega \tau_R} \right)^{1/3} r_s. \tag{51}$$

Note that in writing Eq. (50) a constant of integration has been chosen so as to ensure that islands are ‘‘born’’ in phase with the error-field (i.e.,  $\varphi = 0$  when  $W = 0$ ). The solution (50) is sketched in Fig. 3.

It can be seen from Fig. 3 that driven magnetic islands are ‘‘born’’ in phase with the error-field (as one would expect). However, since the islands are entrained in the plasma flow at the rational surface, they are steadily dragged out of phase. In fact, the islands attain their maximum width,  $W_0$ , when they are in phase quadrature with the error-field (i.e., when  $\varphi = \pi/2$ ). Furthermore, the islands shrink back to zero width by the time they are in antiphase with the error-field (i.e.,  $W \rightarrow 0$  as  $\varphi \rightarrow \pi$ ). Immediately after the antiphase islands disappear they are ‘‘reborn’’ in phase with the error-field, and the process repeats itself *ad infinitum*. Note that the phase difference between the plasma and vacuum islands always lies in the range  $0 \leq \varphi \leq \pi$  (assuming that  $\omega > 0$ ).

Recall, from Sec. III, that in the *linear* regime the reconnected magnetic flux driven by a static error-field in a steadily rotating plasma is small (i.e., much smaller than the ‘‘fully reconnected’’ flux), but *steady* in time. In fact, the phase-shift,  $\varphi$ , between the magnetic perturbation at the rational surface and the error-field is constant. It is clear, from the above, that in the *nonlinear* regime the amount of reconnected magnetic flux *varies periodically* in time, as does the phase shift between the magnetic perturbation at the rational surface and the error-field. This is a direct consequence of the fact that in the nonlinear regime magnetic islands are ‘‘stuck’’ to the plasma (i.e., the plasma cannot flow through them). Hence, if the plasma at the rational surface rotates with respect to the static error-field, the driven magnetic islands must also rotate.

The toroidal electromagnetic torque acting in the vicinity of the rational surface can be written [see Eq. (10)]

$$\delta T_{\phi \text{ EM}} \approx - \frac{8 \pi^2 n m^2 R_0}{\mu_0} \text{Im}(\Delta^{-1}) |\Psi_v|^2. \quad (52)$$

where in the nonlinear regime<sup>5,6</sup>

$$\text{Im}(\Delta^{-1}) = - \frac{1}{2m} \left( \frac{W}{W_v} \right)^2 \sin \varphi. \quad (53)$$

It follows from Eq. (50) and Fig. 3 that in the *Rutherford* regime

$$\text{Im}(\Delta^{-1}) = - \frac{1}{2m} \left( \frac{W_0}{W_v} \right)^2 |\sin \omega t|^{5/3}. \quad (54)$$

It is clear from Eqs. (52) and (54) that in the nonlinear regime the electromagnetic torque acting in the vicinity of the rational surface *pulsates* in time. This behavior is in marked contrast to that found in the linear regime, where the electromagnetic torque is always *constant* in time.

In the following, it is assumed that the plasma is sufficiently viscous that it only responds to the *steady* component of the pulsating electromagnetic torque exerted in the vicinity of the rational surface. This is equivalent to the assumption that the plasma close to the rational surface rotates *uniformly*. This assumption is justified later on. The steady component of Eq. (54) is written

$$\overline{\text{Im}(\Delta^{-1})} = - \frac{0.5356}{2m} \left( \frac{W_0}{W_v} \right)^2, \quad (55)$$

since

$$\frac{1}{\pi} \int_0^\pi (\sin \varphi)^{5/3} d\varphi = 0.5356. \quad (56)$$

The time-averaged, normalized electromagnetic torque acting in the vicinity of the rational surface takes the form

$$\overline{\delta \hat{T}_{\phi \text{ EM}}} = 0.2517 P^{-5/9} Q^{-2/3} R^{-5} \hat{\xi}_s^{5/3}, \quad (57)$$

where use has been made of Eqs. (20), (26), (27), (37), (48), (51), and (55). When this torque is balanced against the normalized viscous torque [see Eq. (36)],

$$\delta \hat{T}_{\phi \text{ VS}} = Q_0 - Q, \quad (58)$$

it is easily demonstrated that the ‘‘downward’’ bifurcation takes place when  $Q = (2/5)Q_0$  (i.e., when the plasma rotation at the rational surface has been reduced to 2/5 of its value in the absence of an error-field). The critical value of  $\hat{\xi}_s$  needed to trigger such a bifurcation is

$$\hat{\xi}_c = 1.167 P^{1/3} Q_0 R^3. \quad (59)$$

The peak normalized width of the driven magnetic island chain at the point of bifurcation is given by

$$\hat{W}_c = 5.541 R. \quad (60)$$

The nonlinear theory presented above is only valid when the width of the magnetic island chain driven at the rational

surface exceeds the linear layer width. The ratio of the peak island width at the bifurcation point to the *visco-resistive* layer width is

$$\frac{\hat{W}_c}{\hat{\delta}_{\text{VR}}} \sim R, \quad (61)$$

where use has been made of Eqs. (28b) and (60). It follows that the plasma resistivity parameter  $R$  [defined in Eq. (24)] can be used as a measure of nonlinearity. If  $R \ll 1$ , then the plasma is sufficiently conductive to ensure that the driven magnetic island width is much less than the linear layer width, in which case linear response theory is valid. On the other hand, if  $R \gg 1$ , then the driven magnetic island width is much greater than the linear layer width, so that nonlinear response theory is valid. The ratio of the peak island width at the bifurcation point to the *resistive-inertial* layer width is

$$\frac{\hat{W}_c}{\hat{\delta}_{\text{RI}}} \sim P^{1/6} Q_0^{-1/4} R, \quad (62)$$

where use has been made of Eq. (29b).

The theory presented above depends crucially on the validity of the constant- $\psi$  approximation. This approximation breaks down when

$$\Delta \frac{W}{r_s} \geq 1. \quad (63)$$

It is easily demonstrated that

$$\Delta \frac{W_c}{r_s} \sim 3.369 P^{1/3} Q_0 R^2 \quad (64)$$

at the point of bifurcation. Hence, the constant- $\psi$  approximation is valid provided that

$$Q_0 \ll P^{-1/3} R^{-2}. \quad (65)$$

Finally, the theory presented above is premised on the assumption that the plasma in the vicinity of the rational surface rotates uniformly, despite the fact that it is subject to a time-varying electromagnetic torque. As is easily demonstrated, this is a reasonable approximation provided that<sup>6</sup>

$$\sqrt{\omega_0 \tau_V} \gg 1, \quad (66)$$

as is likely to be the case in all conventional tokamak plasmas.

### C. The Waelbroeck regime

It is easily shown that in the *Rutherford* regime

$$\Delta \frac{W}{r_s} \sim \frac{\xi_s}{W}. \quad (67)$$

It follows that this nonlinear constant- $\psi$  regime (which is only valid when  $\Delta W/r_s \ll 1$ ) corresponds to the limit in which the ideal plasma displacement at the rational surface,  $\xi_s$ , is much less than the island width,  $W$ . The opposite limit,

$$\xi_s \gtrsim W, \quad (68)$$

in which the displacement exceeds the island width and the constant- $\psi$  approximation breaks down, has been investigated extensively by Waelbroeck.<sup>18-20</sup>

The radial plasma displacement  $\xi(x) = -\psi(x)/sB_\theta(r_s)x$  can be split into components which are even and odd (in  $x$ ) across the rational surface. The even component is trivial:  $\xi(x) = \xi_s/2$ . The odd component has the asymptotic form

$$\xi(x) \rightarrow \frac{1}{2} \left( \text{sgn}(x)\xi_s + \frac{\xi_0}{x} \right) \tag{69}$$

at the edge of the island chain. Here,  $\xi_0$  is related to the parameter  $\Psi_s$ , defined in Eq. (19a), via

$$\Psi_s = -\frac{sB_\theta(r_s)\xi_0}{2}. \tag{70}$$

Furthermore, the quantity  $\Delta$ , which parametrizes the response of the island chain to the error-field, is given by

$$\Delta = \frac{2\xi_s}{\xi_0}. \tag{71}$$

Ideal force balance in the island region yields

$$\nabla^2\psi = I(\psi). \tag{72}$$

According to Waelbroeck,

$$\psi_s \sim IW^2, \tag{73}$$

and

$$\frac{\xi_0}{r_s} \sim \frac{I\psi_s}{[B_\theta(r_s)]^2} \sim \frac{I^2W^2}{[B_\theta(r_s)]^2}. \tag{74}$$

Here,  $\psi_s$  is the true reconnected magnetic flux (i.e., the magnetic flux trapped inside the island separatrix),  $I$  is the typical value of  $I(\psi)$  within the separatrix, and  $W$  is the typical radial extent of the reconnected region.

Suppose that the typical plasma current density inside the island chain is  $\alpha$  times the local equilibrium current density, so that

$$I \sim \alpha \frac{B_\theta(r_s)}{r_s}. \tag{75}$$

It follows from Eqs. (71), (73), and (74) that

$$\frac{\xi_0}{r_s} \sim \alpha^2 \frac{W^2}{r_s^2}, \tag{76}$$

and

$$\Delta \sim \frac{(\xi_s/r_s)}{\alpha^2(W/r_s)^2}. \tag{77}$$

In this paper, it is postulated that

$$\Delta \frac{W}{r_s} \sim 1 \tag{78}$$

in the *Waelbroeck* regime. There are two main justifications for this assumption. The first is by analogy with the linear regime, where it is found that  $\Delta \delta_s/r_s \sim 1$  in all nonconstant- $\psi$  regimes (see Sec. III E). The second is that only by adopting Eq. (78) is it possible to smoothly match

the *Waelbroeck* regime to the *inertial* and *visco-inertial* regimes at high ‘‘slip frequency’’ (see Sec. IV E).

Equations (77) and (78) yield

$$\alpha = \sqrt{\frac{\xi_s}{W}}. \tag{79}$$

It follows that in the *Waelbroeck* regime the plasma current density inside the driven magnetic island chain is generally much larger than the local equilibrium plasma current density. Furthermore, it is easily demonstrated that

$$\Delta^{-1} \sim \frac{W}{r_s}, \tag{80a}$$

$$\psi_s \sim r_s B_\theta(r_s) \left( \frac{\xi_s}{r_s} \right)^{1/2} \left( \frac{W}{r_s} \right)^{3/2}, \tag{80b}$$

$$\psi_s = \sqrt{\frac{W}{\xi_s}} \Psi_s. \tag{80c}$$

According to Eq. (80c), the true reconnected flux,  $\psi_s$ , is generally much less than the parameter  $\Psi_s$  in the *Waelbroeck* regime. By contrast,  $\psi_s = \Psi_s$  in the *Rutherford* regime.

Note that, although the current density inside the island separatrix exceeds the local equilibrium current density, in the *Waelbroeck* regime, most of the current flowing in the vicinity of the rational surface flows in a thin sheet centered on the separatrix. In fact, it is easily demonstrated that the fraction of the total current flowing inside the separatrix, as opposed to in the current sheet, is

$$f \sim \sqrt{\frac{W}{\xi_s}}. \tag{81}$$

Recall that in the nonlinear regime the plasma in the vicinity of the rational surface is required to *corotate* with the magnetic island chain, since plasma is trapped inside the magnetic separatrix. Moreover, it is safe to assume that the plasma close to the rational surface rotates *uniformly*, provided that the inequality (66) is satisfied (as is likely to be the case in all conventional tokamak plasmas<sup>6</sup>). It follows that the helical phase-shift,  $\varphi(t)$ , between the *O*-points of the plasma and vacuum island chains increases *linearly* with time. In other words,

$$\varphi = \omega t, \tag{82}$$

where  $\omega$  is the ‘‘slip frequency.’’ The expected time variation of the phase shift,  $\varphi$ , and the width,  $W$ , of the driven magnetic island chain in the *Waelbroeck* regime is similar to that sketched in Fig. 3. The driven magnetic islands are ‘‘born’’ in phase with the error-field, but are steadily dragged out of phase by the rotating plasma at the rational surface. The islands attain their maximum width,  $W_0$ , when they are approximately in phase quadrature with the error-field. The islands shrink back to zero width by the time they are in antiphase with the error-field. Immediately after the antiphase islands disappear they are ‘‘reborn’’ in phase with the error-field, and the process repeats itself *ad infinitum*.

There is, unfortunately, no equivalent to the Rutherford island evolution equation, (47), in the *Waelbroeck* regime. The best one can do is to estimate the peak reconnected flux,  $\psi_s$ , using the *Sweet–Parker* model, which allows one to make a crude prediction of the rate of magnetic reconnection,  $\dot{\psi}_s$ , when the helical phase-shift between the plasma and vacuum islands,  $\varphi$ , is zero. The estimate for the peak reconnected flux is then simply

$$\psi_s \sim \omega^{-1} \dot{\psi}_s. \quad (83)$$

The *Sweet–Parker* prediction for the reconnection rate in the *Waelbroeck* regime is<sup>21–23</sup>

$$\dot{\psi}_s \sim r_s B_\theta(r_s) \frac{(\xi_s/r_s)^{3/2}}{\tau_H^{1/2} \tau_R^{1/2} (1 + \tau_R/\tau_V)^{1/4}}. \quad (84)$$

It follows from Eq. (83) that the peak reconnected flux is given by

$$\psi_s \sim r_s B_\theta(r_s) \frac{(\xi_s/r_s)^{3/2}}{\omega \tau_H^{1/2} \tau_R^{1/2} (1 + \tau_R/\tau_V)^{1/4}}. \quad (85)$$

Finally, according to Eq. (80b), the peak magnetic island width,  $W_0$ , can be written

$$W_0 \sim \frac{(\xi_s/r_s)^{2/3}}{\omega^{2/3} \tau_H^{1/3} \tau_R^{1/3} (1 + \tau_R/\tau_V)^{1/6}} r_s. \quad (86)$$

As in the *Rutherford* regime, in the *Waelbroeck* regime the electromagnetic torque acting in the vicinity of the rational surface *pulsates* in time. However, provided the inequality (66) is satisfied, the plasma is sufficiently viscous that it only responds to the *steady* component of the torque. According to Eqs. (37) and (80a), the normalized, steady component of the electromagnetic torque acting in the vicinity of the rational surface is given by

$$\overline{\delta \hat{T}}_{\phi \text{ EM}} \sim P^{-1/3} R^{-5} \hat{W}_0 \hat{\xi}_s^2. \quad (87)$$

Note that the electromagnetic torque in the *Waelbroeck* regime can only be evaluated to within an unknown, positive,  $O(1)$  (hopefully!), multiplicative constant, because of the essentially heuristic nature of the *Sweet–Parker* model.

Equations (86) and (87) can be combined to give the following expression for the normalized electromagnetic torque acting in the vicinity of the rational surface:

$$\overline{\delta \hat{T}}_{\phi \text{ EM}} \sim P^{-7/18} (1 + P)^{-1/6} Q_0^{-2/3} R^{-5} \hat{\xi}_s^{8/3}. \quad (88)$$

When this torque is balanced against the normalized viscous torque [see Eq. (36)], it is easily demonstrated that the ‘‘downward’’ bifurcation takes place when  $Q = (2/5)Q_0$  (i.e., when the plasma rotation at the rational surface has been reduced to 2/5 of its value in the absence of an error-field). The critical value of  $\hat{\xi}_s$  needed to trigger such a bifurcation is

$$\hat{\xi}_c \sim P^{7/48} (1 + P)^{1/16} Q_0^{5/8} R^{15/8}. \quad (89)$$

Note that this result differs from that of Bhattacharjee and co-workers, who assumed that  $\psi_s \sim \Psi_s$  in the nonlinear

nonconstant- $\psi$  regime.<sup>8</sup> The peak normalized width of the driven magnetic island chain at the point of bifurcation is given by

$$\hat{W}_c \sim P^{1/24} (1 + P)^{-1/8} Q_0^{-1/4} R^{5/4}. \quad (90)$$

The theory presented above depends crucially on the breakdown of the constant- $\psi$  approximation. According to Eq. (68), the constant- $\psi$  approximation breaks down at the bifurcation point whenever

$$\hat{\xi}_c \gtrsim \hat{W}_c. \quad (91)$$

It follows from Eqs. (89) and (90) that the *Waelbroeck* regime holds as long as

$$Q_0 \gtrsim P^{-5/42} (1 + P)^{-3/14} R^{-5/7}. \quad (92)$$

#### D. The transition regime

According to Eqs. (65) and (92), in the nonlinear limit the *Rutherford* regime holds whenever  $Q_0 < Q_a$ , where

$$Q_a \sim P^{-1/3} R^{-2}, \quad (93)$$

and the *Waelbroeck* regime holds whenever  $Q_0 > Q_b$ , where

$$Q_b \sim P^{-5/42} (1 + P)^{-3/14} R^{-5/7}. \quad (94)$$

It is easily seen that  $Q_b > Q_a$  for

$$R > R_c = (1 + P^{-1})^{1/6}. \quad (95)$$

It turns out that  $R < R_c$  corresponds to the linear limit. Thus, in the nonlinear limit (i.e.,  $R > R_c$ ) there is a ‘‘transition regime,’’ linking the *Rutherford* and *Waelbroeck* regimes, which extends over the range of normalized plasma rotation frequencies  $Q_a \lesssim Q_0 \lesssim Q_b$ .

The *transition* regime exists because the rate of magnetic reconnection in the *Waelbroeck* regime is far larger than that in the *Rutherford* regime, so if the reconnection rate is to vary continuously with the normalized plasma rotation frequency,  $Q_0$ , as seems reasonable, then there needs to be an intermediate regime, linking the *Rutherford* and *Waelbroeck* regimes, in which the reconnection rate gradually accelerates from the typical *Rutherford* rate to the typical *Waelbroeck* rate.

In the *Rutherford* regime, the plasma displacement,  $\xi_s$ , is much less than the island width,  $W$ , the parameter  $\alpha$  [i.e., the ratio of the typical helical current density inside the island chain to the local equilibrium current density: see Eq. (75)] is much less than unity, the typical plasma velocity associated with magnetic reconnection is  $v_* \sim \omega r_s$ , and the width of the reconnecting region is the island width,  $W$ . By contrast, in the *Waelbroeck* regime, the plasma displacement,  $\xi_s$ , is much greater than the island width,  $W$ ; the parameter  $\alpha$  is much greater than unity [see Eq. (79)]; the typical plasma velocity associated with magnetic reconnection is

$$v_* \sim \frac{r_s}{\tau_H} (1 + \tau_R/\tau_V)^{-1/2} \frac{\xi_s}{r_s} \quad (96)$$

(this is the exit velocity of plasma from the *Sweet–Parker* layer<sup>23</sup>); and the width of the reconnecting region is

$$\delta \sim \sqrt{\frac{\tau_H}{\tau_R}} (1 + \tau_R/\tau_V)^{1/4} \sqrt{\frac{r_s}{\xi_s}} r_s \quad (97)$$

(this is the width of the Sweet–Parker layer<sup>23</sup>).

It is plausible that in the *transition* regime

$$\xi_s \sim W \quad (98)$$

(i.e., the plasma displacement is of order the island width, which implies that the *transition* regime is a nonconstant- $\psi$  regime), and

$$\alpha \sim 1 \quad (99)$$

(i.e., the helical current density inside the island is of order the local equilibrium current density). It follows from Eq. (77) that

$$\Delta \frac{W}{r_s} \sim 1 \quad (100)$$

in the *transition* region. This is a particular case of what appears to be a more general rule. Namely,  $\Delta \delta_s/r_s \sim 1$  in all linear nonconstant- $\psi$  regimes (where  $\delta_s$  is the linear layer width), and  $\Delta W/r_s \sim 1$  in all nonlinear nonconstant- $\psi$  regimes (where  $W$  is the island width).

Suppose that the typical plasma velocity associated with magnetic reconnection in the *transition* regime is

$$v_* \sim \beta \frac{r_s}{\tau_H} (1 + \tau_R/\tau_V)^{-1/2} \frac{\xi_s}{r_s} \quad (101)$$

(this is the exit velocity of plasma from the modified Sweet–Parker layer), where  $\beta \leq 1$ . Using similar arguments to those employed by Park *et al.*,<sup>23</sup> the width of the reconnecting region is

$$\delta \sim \frac{1}{\sqrt{\beta}} \sqrt{\frac{\tau_H}{\tau_R}} (1 + \tau_R/\tau_V)^{1/4} \sqrt{\frac{r_s}{\xi_s}} r_s \quad (102)$$

(this is the width of the modified Sweet–Parker layer), and the reconnection rate is given by

$$\dot{\psi}_s \sim r_s B_{\theta}(r_s) \frac{\sqrt{\beta}}{\tau_H^{1/2} \tau_R^{1/2} (1 + \tau_R/\tau_V)^{1/4}} \left(\frac{\xi_s}{r_s}\right)^{3/2}. \quad (103)$$

Thus, in the *transition* regime the plasma velocity associated with magnetic reconnection is less than that in the *Waelbroeck* regime. Consequently, the width of the reconnecting region is greater than that in the *Waelbroeck* regime, and the reconnection rate is reduced.

As in the *Rutherford* and *Waelbroeck* regimes, in the *transition* regime the reconnected magnetic flux pulsates at the slip frequency,  $\omega$ . It follows that the peak reconnected flux is given by [see Eq. (83)]

$$\psi_s \sim \omega^{-1} \dot{\psi}_s \sim r_s B_{\theta}(r_s) \frac{\sqrt{\beta}}{\omega \tau_H^{1/2} \tau_R^{1/2} (1 + \tau_R/\tau_V)^{1/4}} \left(\frac{\xi_s}{r_s}\right)^{3/2}. \quad (104)$$

According to Eq. (80b), the peak magnetic island width,  $W_0$ , can be written

$$W_0 \sim \frac{\beta^{1/3}}{[\omega \tau_H^{1/2} \tau_R^{1/2} (1 + \tau_R/\tau_V)^{1/4}]^{2/3}} \left(\frac{\xi_s}{r_s}\right)^{2/3} r_s. \quad (105)$$

Now,  $\xi_s \sim W_0$  in the *transition* region [see Eq. (98)]. Hence, the above expression yields

$$\beta \sim [\omega \tau_H^{1/2} \tau_R^{1/2} (1 + \tau_R/\tau_V)^{1/4}]^2 \frac{\xi_s}{r_s}, \quad (106a)$$

$$v_* \sim r_s \omega^2 \tau_R \left(\frac{\xi_s}{r_s}\right)^2, \quad (106b)$$

$$\frac{\delta}{W_0} \sim \frac{1}{\omega \tau_R} \left(\frac{r_s}{\xi_s}\right)^2, \quad (106c)$$

where use has been made of Eqs. (101) and (102).

As before, the electromagnetic torque acting in the vicinity of the rational surface *pulsates* in time. However, the plasma is assumed to be sufficiently viscous that it only responds to the steady component of this torque. According to Eqs. (37), (98), and (100), the normalized, steady component of the electromagnetic torque acting in the vicinity of the rational surface is given by

$$\overline{\delta \hat{T}_{\phi \text{ EM}}} \sim P^{-1/3} R^{-5} \hat{\xi}_s^3. \quad (107)$$

Note that the torque is independent of the normalized plasma rotation frequency,  $Q_0$ , at constant normalized error-field strength,  $\hat{\xi}_s$ . When this torque is balanced against the normalized viscous torque [see Eq. (36)], it is easily demonstrated that the “downward” bifurcation takes place at  $Q \sim Q_a$  (i.e., when the plasma rotation at the rational surface has been reduced to such a level that the plasma is just about to leave the *transition* regime and enter the *Rutherford* regime). The critical value of  $\xi_s$  needed to trigger such a bifurcation (assuming that  $Q_a \ll Q_0$ ) is

$$\hat{\xi}_c \sim P^{1/9} Q_0^{1/3} R^{5/3}. \quad (108)$$

Since  $\xi_s \sim W_0$  in the *transition* regime, the peak normalized width of the driven magnetic island chain at the point of bifurcation is

$$\hat{W}_c \sim P^{1/9} Q_0^{1/3} R^{5/3}. \quad (109)$$

In the *transition* regime, the width of the reconnecting region can be less than the island width (corresponding to the presence of a Sweet–Parker-like reconnecting layer), but it cannot be greater than the island width. The inequality

$$\delta < W_0 \quad (110)$$

reduces to

$$Q_0 > Q_a \sim P^{-1/3} R^{-2}, \quad (111)$$

with the aid of Eqs. (106c) and (108). In fact, as  $Q_0 \rightarrow Q_a$ , the plasma velocity associated with reconnection, the width of the reconnecting region, and the rate of reconnection in the *transition* regime all asymptote smoothly to the values appropriate to the *Rutherford* regime.

In the *transition* regime, the velocity associated with reconnection cannot exceed that in the *Waelbroeck* regime (since this velocity is an upper limit). The inequality

$$\beta < 1 \quad (112)$$

reduces to

$$Q_0 < Q_b \sim P^{-5/42}(1+P)^{-3/14}R^{-5/7}, \quad (113)$$

with the aid of Eqs. (106a) and (108). In fact, as  $Q_0 \rightarrow Q_b$ , the plasma velocity associated with reconnection, the width of the reconnecting region, and the rate of reconnection in the *transition* regime all asymptote smoothly to the values appropriate to the *Waelbroeck* regime.

### E. The non-reconnecting regimes

As the plasma resistivity parameter,  $R$ , increases, the amount of driven magnetic reconnection also increases, and the linear constant- $\psi$  plasma response regimes discussed in Sec. III eventually merge into the *Rutherford* regime (see Sect. IV B). The upper boundary of the linear constant- $\psi$  regime (in  $R$ ) corresponds to the point at which the width of the reconnected region (i.e., the width of the driven island chain) becomes comparable with the linear layer width at the rational surface. Note, however, that the linear non-constant- $\psi$  regimes discussed in Sec. III are non-reconnecting (i.e., there is no driven magnetic reconnection in these regimes), so the width of the reconnected region is always *zero* in these regimes. It follows that, unlike the linear constant- $\psi$  regimes, there is no reason why the linear nonconstant- $\psi$  regimes should become invalid in the high resistivity limit,  $R \gg 1$ .

One expects the linear nonconstant- $\psi$  regimes to hold in the high resistivity limit,  $R \gg 1$ , whenever the linear layer width associated with these regimes *exceeds* the magnetic island width predicted by the nonlinear nonconstant- $\psi$  regimes. The normalized linear layer width in the *visco-inertial* regime is given by [see Eq. (30b)]

$$\hat{\delta}_{VI} \sim P^{1/12}Q_0^{1/4}, \quad (114)$$

assuming  $Q \sim Q_0$ . This width exceeds the typical width of the driven magnetic island chain in the *Waelbroeck* regime, given by Eq. (90), when

$$Q_0 > Q_c \sim P^{-1/12}(1+P)^{-1/4}R^{5/2}. \quad (115)$$

The normalized linear layer width in the *inertial* regime is given by [see Eq. (31b)]

$$\hat{\delta}_I \sim P^{-1/6}Q_0, \quad (116)$$

assuming  $Q \sim Q_0$ . This width exceeds the typical width of the driven magnetic island chain in the *Waelbroeck* regime when

$$Q_0 > Q_c \sim P^{1/6}(1+P)^{-1/10}R. \quad (117)$$

Thus, the *Waelbroeck* regime extends over the range of normalized plasma rotation frequencies  $Q_b < Q_0 < Q_c$ , where  $Q_b$  is given by Eq. (94), and  $Q_c$  is the lowest of the two frequencies specified in Eqs. (115) and (117).

The normalized electromagnetic torque acting in the vicinity of the rational surface in the *visco-inertial* regime is given by [see Eq. (40)]

$$\delta \hat{T}_{\phi \text{ EM}} \sim P^{-1/4}Q^{1/4}R^{-5}\hat{\xi}_s^2. \quad (118)$$

When this torque is balanced against the normalized viscous torque [see Eq. (36)], it is easily demonstrated that the “downward” bifurcation takes place when  $Q_0 \sim Q_c$  (i.e.,

when the plasma rotation at the rational surface has been reduced to such a level that the plasma is just about to leave the *visco-inertial* regime and enter the *Waelbroeck* regime). The critical value of  $\hat{\xi}_s$  needed to trigger such a bifurcation is

$$\hat{\xi}_c \sim P^{1/6}(1+P^{-1})^{1/32}Q_0^{1/2}R^{35/16}. \quad (119)$$

The typical normalized linear layer width at the bifurcation point is

$$\hat{\delta}_c \sim (1+P^{-1})^{-1/16}R^{5/8}, \quad (120)$$

where use has been made of Eqs. (30b) and (115).

The normalized electromagnetic torque acting in the vicinity of the rational surface in the *inertial* regime is given by [see Eq. (41)]

$$\delta \hat{T}_{\phi \text{ EM}} \sim P^{-1/2}QR^{-5}\hat{\xi}_s^2. \quad (121)$$

When this torque is balanced against the normalized viscous torque [see Eq. (36)], it is easily demonstrated that the “downward” bifurcation takes place when  $Q_0 \sim Q_c$  (i.e., when the plasma rotation at the rational surface has been reduced to such a level that the plasma is just about to leave the *inertial* regime and enter the *Waelbroeck* regime). The critical value of  $\hat{\xi}_s$  needed to trigger such a bifurcation is

$$\hat{\xi}_c \sim P^{1/6}(1+P)^{1/20}Q_0^{1/2}R^2. \quad (122)$$

The typical normalized linear layer width at the bifurcation point is

$$\hat{\delta}_c \sim (1+P)^{-1/10}R, \quad (123)$$

where use has been made of Eqs. (31b) and (117).

### F. The “downward” bifurcation

It is now possible to present a *fully comprehensive theory* describing the “downward” bifurcation of a rotating tokamak plasma interacting with a static, resonant error-field: i.e., the error-field-induced bifurcation from the “unreconnected” state, in which the plasma at the rational surface rotates with respect to the error-field and there is comparatively little driven magnetic reconnection, to the “fully reconnected” state, in which the plasma rotation at the rational surface is arrested and driven reconnection proceeds without hindrance.

Figure 4 shows the extents of the various plasma response regimes for the “downward” bifurcation plotted in normalized plasma resistivity,  $R$ , versus normalized plasma rotation,  $Q_0$ , space, in the limit of high plasma viscosity,  $P \gg 1$ . There are *seven* different regimes. Namely, the *visco-resistive* regime (VR), the *Rutherford* regime (R), the *transition* regime (T), the *Waelbroeck* regime (W), the *inertial* regime (I), the *high-resistivity visco-inertial* regime (VI<sub>+</sub>), and the *low-resistivity visco-inertial* regime (VI<sub>-</sub>). The *visco-resistive* and *low-resistivity visco-inertial* regimes are identical to the *visco-resistive* (VR) and *visco-inertial* (VI) regimes shown in Fig. 2. In fact, Fig. 2 can be regarded as the low resistivity (i.e.,  $R \ll 1$ ) limit of Fig. 4.

In the *visco-resistive* regime, the critical error-field amplitude needed to trigger a “downward” bifurcation, and the linear layer width at the bifurcation point, are given by

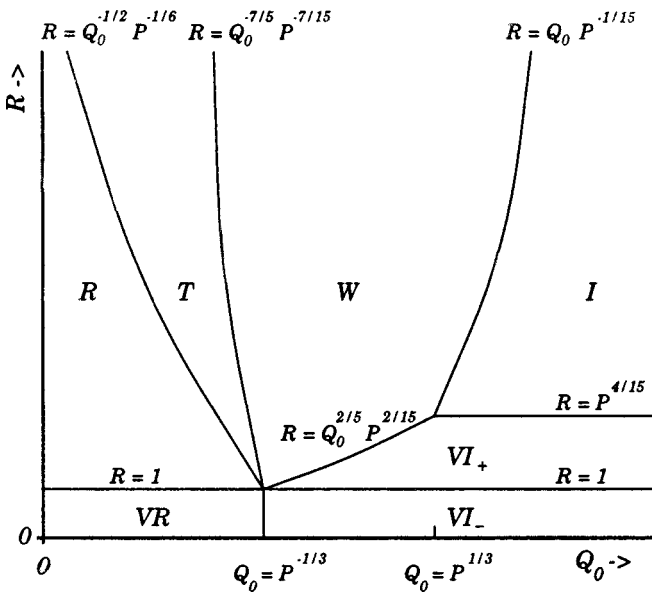


FIG. 4. A schematic diagram showing the extents of the various “downward” bifurcation regimes plotted in normalized plasma resistivity,  $R$ , versus normalized plasma rotation,  $Q_0$ , space, in the high-plasma-viscosity limit,  $P \gg 1$ . The seven regimes are the *visco-resistive* regime (VR), the *Rutherford* regime (R), the *transition* regime (T), the *Waelbroeck* regime (W), the *inertial* regime (I), the *high-resistivity visco-inertial* regime ( $VI_+$ ), and the *low-resistivity visco-inertial* regime ( $VI_-$ ).

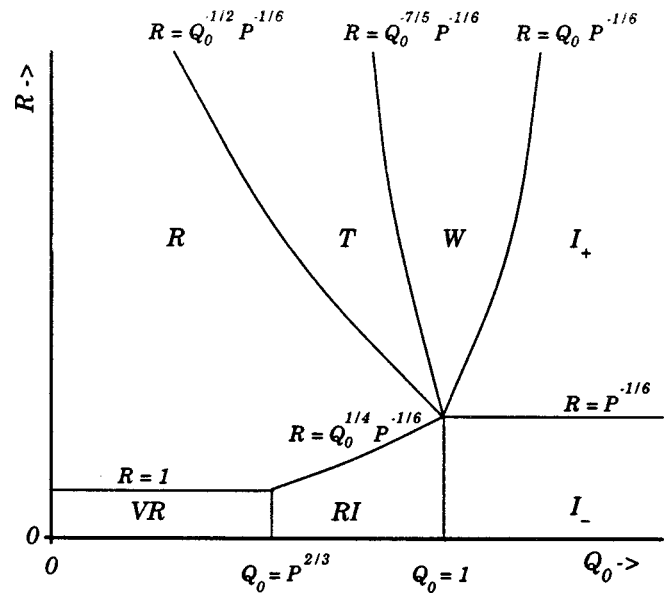


FIG. 5. A schematic diagram showing the extents of the various “downward” bifurcation regimes plotted in normalized plasma resistivity,  $R$ , versus normalized plasma rotation,  $Q_0$ , space, in the low-plasma-viscosity limit,  $P \ll 1$ . The seven regimes are the *visco-resistive* regime (VR), the *resistive-inertial* regime (RI), the *Rutherford* regime (R), the *transition* regime (T), the *Waelbroeck* regime (W), the *high-resistivity inertial* regime ( $I_+$ ), and the *low-resistivity inertial* regime ( $I_-$ ).

$$\hat{\xi}_c \sim P^{1/3} Q_0 R^{5/2}, \tag{124a}$$

$$\hat{\delta}_c \sim 1, \tag{124b}$$

respectively.

In the *Rutherford* regime, the critical error-field amplitude needed to trigger a “downward” bifurcation, and the magnetic island width at the bifurcation point, are given by

$$\hat{\xi}_c \sim P^{1/3} Q_0 R^3, \tag{125a}$$

$$\hat{W}_c \sim R, \tag{125b}$$

respectively.

In the *transition* regime, the critical error-field amplitude needed to trigger a “downward” bifurcation, and the magnetic island width at the bifurcation point, are given by

$$\hat{\xi}_c \sim P^{1/9} Q_0^{1/3} R^{5/3}, \tag{126a}$$

$$\hat{W}_c \sim P^{1/9} Q_0^{1/3} R^{5/3}, \tag{126b}$$

respectively.

In the *Waelbroeck* regime, the critical error-field amplitude needed to trigger a “downward” bifurcation, and the magnetic island width at the bifurcation point, are given by

$$\hat{\xi}_c \sim P^{5/24} Q_0^{5/8} R^{15/8}, \tag{127a}$$

$$\hat{W}_c \sim P^{-1/12} Q_0^{-1/4} R^{5/4}, \tag{127b}$$

respectively.

In the *inertial* regime, the critical error-field amplitude needed to trigger a “downward” bifurcation, and the linear layer width at the bifurcation point, are given by

$$\hat{\xi}_c \sim P^{13/60} Q_0^{1/2} R^2, \tag{128a}$$

$$\hat{\delta}_c \sim P^{-1/10} R, \tag{128b}$$

respectively.

In the *high-resistivity visco-inertial* regime, the critical error-field amplitude needed to trigger a “downward” bifurcation, and the linear layer width at the bifurcation point, are given by

$$\hat{\xi}_c \sim P^{1/6} Q_0^{1/2} R^{35/16}, \tag{129a}$$

$$\hat{\delta}_c \sim R^{5/8}, \tag{129b}$$

respectively.

Finally, in the *low-resistivity visco-inertial* regime, the critical error-field amplitude needed to trigger a “downward” bifurcation, and the linear layer width at the bifurcation point, are given by

$$\hat{\xi}_c \sim P^{1/6} Q_0^{1/2} R^{5/2}, \tag{130a}$$

$$\hat{\delta}_c \sim 1, \tag{130b}$$

respectively.

Figure 5 shows the extents of the various plasma response regimes for the “downward” bifurcation plotted in normalized plasma resistivity,  $R$ , versus normalized plasma rotation,  $Q_0$ , space, in the limit of low plasma viscosity,  $P \ll 1$ . There are seven different regimes. Namely, the *visco-resistive*, *resistive-inertial*, and *low-resistivity inertial* regimes (VR, RI, and  $I_-$ ), the *Rutherford* regime (R), the *transition* regime (T), the *Waelbroeck* regime (W), the *high-resistivity inertial* regime ( $I_+$ ), and the *low-resistivity inertial* regime ( $I_-$ ). The *visco-resistive*, *resistive-inertial*, and *low-resistivity inertial* regimes

gimes are identical to the *visco-resistive* (VR), *resistive-inertial* (RI), and *inertial* (I) regimes shown in Fig. 2. In fact, Fig. 2 can be regarded as the low resistivity (i.e.,  $R \ll 1$ ) limit of Fig. 5.

In the *visco-resistive* regime, the critical error-field amplitude needed to trigger a “downward” bifurcation, and the linear layer width at the bifurcation point, are given by Eqs. (124).

$$\hat{\xi}_c \sim P^{1/4} Q_0^{9/8} R^{5/2}, \quad (131a)$$

$$\hat{\delta}_c \sim P^{-1/6} Q_0^{1/4}, \quad (131b)$$

respectively.

In the *Rutherford* regime, the critical error-field amplitude needed to trigger a “downward” bifurcation, and the magnetic island width at the bifurcation point, are given by Eqs. (125).

In the *transition* regime, the critical error-field amplitude needed to trigger a “downward” bifurcation, and the magnetic island width at the bifurcation point, are given by Eqs. (126).

In the *Waelbroeck* regime, the critical error-field amplitude needed to trigger a “downward” bifurcation, and the magnetic island width at the bifurcation point, are given by

$$\hat{\xi}_c \sim P^{7/48} Q_0^{5/8} R^{15/8}, \quad (132a)$$

$$\hat{W}_c \sim P^{1/24} Q_0^{-1/4} R^{5/4}, \quad (132b)$$

respectively.

In the *high-resistivity inertial* regime, the critical error-field amplitude needed to trigger a “downward” bifurcation, and the linear layer width at the bifurcation point, are given by

$$\hat{\xi}_c \sim P^{1/6} Q_0^{1/2} R^2, \quad (133a)$$

$$\hat{\delta}_c \sim R, \quad (133b)$$

respectively.

Finally, in the *low-resistivity inertial* regime, the critical error-field amplitude needed to trigger a “downward” bifurcation, and the linear layer width at the bifurcation point, are given by

$$\hat{\xi}_c \sim P^{1/4} Q_0^{1/2} R^{5/2}, \quad (134a)$$

$$\hat{\delta}_c \sim P^{-1/6}, \quad (134b)$$

respectively.

Note that the critical error-field amplitude,  $\hat{\xi}_c$ , and the layer/island width at the bifurcation point,  $\hat{\delta}_c/\hat{W}_c$ , both vary *continuously* from one regime to another.

The *Rutherford*, *transition*, and *Waelbroeck* regimes are all *nonlinear* response regimes. The remaining regimes are all *linear* response regimes.

The *visco-resistive*, *resistive-inertial*, and *Rutherford* regimes are all *constant- $\psi$*  regimes: i.e.,  $\psi_s/\Psi_s = 1$ , where  $\psi_s$  is the true reconnected magnetic flux, and  $\Psi_s$  is the flux at

the edge of the layer/island [see Eqs. (19)]. The *transition* and *Waelbroeck* regimes are both *nonconstant- $\psi$*  regimes: i.e.,  $\psi_s/\Psi_s \ll 1$ . The remaining regimes are all *non-reconnecting* regimes: i.e.,  $\psi_s/\Psi_s \rightarrow 0$ .

The ideal plasma displacement at the bifurcation point,  $\hat{\xi}_c$ , is much less than the corresponding layer/island width,  $\hat{\delta}_c/\hat{W}_c$ , in the three constant- $\psi$  regimes. The ideal displacement at the bifurcation point is similar to the island width in the *transition* regime. The ideal displacement at the bifurcation point can be either larger or smaller than the layer width in the *low-resistivity visco-resistive* and *low-resistivity inertial* regimes. Finally, the ideal displacement at the bifurcation point is much larger than the corresponding layer/island width in all of the remaining regimes.

## G. The “upward” bifurcation

Consider the “upward” bifurcation of a rotating tokamak plasma interacting with a static, resonant error-field: i.e., the error-field-induced bifurcation from the “fully reconnected” state, in which the plasma rotation at the rational surface is arrested and driven magnetic reconnection proceeds without hindrance, to the “unreconnected” state, in which the plasma at the rational surface rotates with respect to the error-field and there is comparatively little driven reconnection.

The “upward” bifurcation depends solely on the properties of the “fully reconnected” plasma state, in which there is no plasma rotation at the rational surface (i.e., the “slip frequency,”  $\omega$ , is zero), and  $|\Delta| \sim (-\Delta') \sim O(1)$ . In this state, the amount of driven magnetic reconnection approaches close to the theoretical maximum value, leading inevitably to the formation of a locked Rutherford island chain at the rational surface. It is easily demonstrated, from the analysis of Sec. IV B, that the steady-state width of this locked island chain is given by

$$W = \sqrt{\frac{2m \cos \varphi}{-\Delta'}} W_v, \quad (135)$$

where  $W_v$  is the width of the “vacuum island” chain, and  $\varphi$  is the *steady* helical phase shift between the  $O$ -points of the plasma and vacuum island chains. The *steady* electromagnetic torque exerted in the vicinity of the rational surface takes the form

$$\delta T_{\phi \text{ EM}} = \frac{4\pi^2 n m^2 R_0}{\mu_0 (-\Delta')} |\Psi_v|^2 \sin 2\varphi, \quad (136)$$

where  $\Psi_v$  is the “vacuum flux.”

When written in normalized form, the above electromagnetic torque reduces to

$$\delta \hat{T}_{\phi \text{ EM}} = \frac{(-\Delta')^{-1}}{4} P^{-1/2} R^{-5} S^{1/3} \hat{\xi}_s^2 \sin 2\varphi, \quad (137)$$

where

$$S = \frac{\tau_R}{\tau_H} \quad (138)$$

is the Lundquist number of the plasma. When this torque is balanced against the normalized viscous torque, which takes the form

$$\delta \hat{T}_{\phi} \nu_S = Q_0 \quad (139)$$

for a locked island chain, it is easily demonstrated that the bifurcation to the “unreconnected” branch of solutions takes place when the helical phase shift,  $\varphi$ , between the plasma and vacuum islands exceeds a critical value of  $45^\circ$ .<sup>6</sup> The critical value of  $\hat{\xi}_s$  below which this bifurcation takes place is

$$\hat{\xi}_c = 2(-\Delta')^{1/2} P^{1/4} Q_0^{1/2} R^{5/2} S^{-1/6}. \quad (140)$$

The normalized width of the driven island chain at the bifurcation point is

$$\hat{W}_c = 4.757(-\Delta')^{-1/4} P^{1/24} Q_0^{1/4} R^{5/4} S^{1/12}. \quad (141)$$

Broadly speaking, the nondimensional parameters  $P$ ,  $Q_0$ , and  $R$  are  $O(1)$  in conventional tokamak plasmas, whereas the parameter  $S$  is much greater than unity (see Sec. V). It follows from a comparison of Eqs. (124)–(134) and Eqs. (140) and (141) that the critical error-field amplitude needed to trigger a “downward” bifurcation of the plasma is significantly larger than the critical amplitude needed to trigger an “upward” bifurcation: i.e., there is a significant “hysteresis” effect associated with error-field-driven magnetic reconnection. Furthermore, the typical magnetic island width in the “fully reconnected” plasma state is significantly larger than the layer/island width in the “unreconnected” state.

## V. APPLICATION TO EXPERIMENTS

### A. Plasma rotation

Tokamak plasmas rotate for many different reasons. Some tokamaks are heated by unbalanced neutral beam injection (NBI), in which high energy (e.g., 75 keV) neutral particles are injected into the plasma preferentially in one toroidal direction. Although this is primarily a heating scheme, it gives rise to bulk toroidal plasma rotation with velocities typically in excess of  $10 \text{ km s}^{-1}$ .<sup>24,25</sup> In ohmically heated tokamaks, where there is little or no bulk plasma rotation, the “natural frequencies” of tearing modes are still nonzero because of plasma diamagnetism. In fact, tearing modes in ohmically heated tokamaks are observed to rotate in the electron direction (i.e., in the same sense as the electrons which carry the equilibrium toroidal current) with velocities which are of order the electron diamagnetic velocity.<sup>26</sup> Thus, a good estimate for the “natural frequency” of a tearing mode in an ohmic tokamak is

$$\omega_0 \sim \frac{m T_e(r_s)(\eta_{n_e} + \eta_{T_e})}{e B_\phi r_s^2}, \quad (142)$$

where  $T_e$  is the electron temperature,  $n_e$  is the electron number density,  $\eta_{n_e} = -(d \ln n_e / d \ln r)_{r_s}$ , and  $\eta_{T_e} = -(d \ln T_e / d \ln r)_{r_s}$ . Note that the “natural frequencies” of tearing modes in NBI-heated plasmas are generally, at least, an order of magnitude higher than the above estimate.

TABLE I. The Lundquist number ( $S$ ), the plasma viscosity parameter ( $P$ ), the plasma rotation parameter ( $Q_0$ ), and the plasma resistivity parameter ( $R$ ) estimated as functions of the major radius ( $R_0$ ) for typical low-density, ohmically heated target plasmas in JET-like tokamaks. Also shown is the critical value,  $Q_a$ , of the plasma rotation parameter above which the constant- $\psi$  approximation breaks down. The final column gives the critical 2.1 vacuum radial error-field at the rotational surface required to trigger a “downward” bifurcation of the plasma state as a fraction of the toroidal field-strength.

$R_0$	$S$	$P$	$Q_0$	$R$	$Q_a$	$b_r / B_\phi$
0.5	$1.6 \times 10^5$	1.7	0.42	1.33	0.473	$3.2 \times 10^{-3}$
1.0	$1.4 \times 10^6$	2.3	0.33	1.16	0.563	$9.2 \times 10^{-4}$
1.5	$4.8 \times 10^6$	2.7	0.28	1.07	0.623	$4.5 \times 10^{-4}$
2.0	$1.2 \times 10^7$	3.0	0.25	1.02	0.669	$2.7 \times 10^{-4}$
2.5	$2.4 \times 10^7$	3.3	0.23	0.973	0.670	$1.8 \times 10^{-4}$
3.0	$4.1 \times 10^7$	3.6	0.22	0.939	0.653	$1.3 \times 10^{-4}$
8.0	$8.8 \times 10^8$	5.4	0.15	0.776	0.570	$2.5 \times 10^{-5}$

Note, from Eq. (142), that  $\omega_0 \propto T_e / (B_\phi a^2)$  for similar ohmic plasma discharges in different devices. This suggests that the “natural frequencies” of tearing modes in ohmically heated tokamaks are *strongly decreasing* functions of the dimensions of the device (the variation of  $T_e / B_\phi$  with machine size is relatively weak). Now, in all plasma response regimes mentioned in Sec. IV, the critical error-field needed to trigger a “downward” bifurcation of the plasma state, and, thereby, enable error-field-driven magnetic reconnection, is an *increasing* function of the “natural frequency,”  $\omega_0$ . It follows that large ohmically heated tokamaks are likely to be *far more susceptible* to error-field-driven reconnection, and the associated degradation of plasma confinement, than small tokamaks.

### B. Scaling of the critical error-field with machine size

The aim of this section is to estimate the critical  $m = 2/n = 1$  error-field amplitude required to induce a “downward” bifurcation of the plasma state in a low density, ohmic target plasma as a function of machine size. Consider the family of JET-like (JET stands for “Joint European Torus”) tokamaks for which

$$a = 0.35 R_0, \quad (143)$$

and

$$B_\phi = 1.38 R_0^{0.7}, \quad (144)$$

Broadly speaking, most modern tokamaks of conventional design are members of this family (e.g., COMPASS-C,<sup>27</sup> DIII-D,<sup>28</sup> and JET<sup>29</sup>). The discharge parameters for low density (i.e., a line-integrated electron number density of  $2 \times 10^{19} \text{ m}^{-3}$ ) ohmically heated plasmas can be estimated using the simple scaling model described in Sect. 8 and Appendix B of Ref. 6. Table I shows the Lundquist number,  $S$  [defined in Eq. (138)], the plasma viscosity parameter,  $P$  [defined in Eq. (23)], the plasma rotation parameter,  $Q_0$  [defined in Eq. (22)], and the plasma resistivity parameter,  $R$  [defined in Eq. (24)], estimated as functions of the major radius,  $R_0$ . Also shown is  $Q_a$ : the critical value of  $Q_0$  above which the constant- $\psi$  approximation breaks down in the vi-

cinity of the rational surface. It can be seen that  $P$ ,  $Q_0$ , and  $R$  are  $O(1)$  parameters, whereas  $S \gg 1$ , in accordance with the assumption made in Sec. IV G. Note that  $P > 1$ , indicating that the plasma response regime at the rational surface is determined by Fig. 4. Thus,

$$Q_a = \begin{cases} P^{-1/3} & \text{for } R \leq 1 \\ P^{-1/3} R^{-2} & \text{for } R > 1 \end{cases} \quad (145)$$

The parameter  $R$  is effectively a measure of nonlinearity. For  $R < 1$ , linear response theory is valid, but for  $R > 1$ , linear response theory breaks down, and nonlinear response theory takes over. It can be seen from Table I that in small tokamaks the response of the plasma to the error-field is nonlinear, whereas in large tokamaks the response is linear. Furthermore, although the constant- $\psi$  approximation is on the verge of breaking down in small tokamaks, it remains a good approximation in large tokamaks. Thus, the appropriate response regime for the plasma at the rational surface is the *Rutherford* regime for small tokamaks, and the *visco-resistive* regime for large tokamaks. In particular, the appropriate response regime for a reactor-sized tokamak (i.e.,  $R_0 \sim 8$  m) is undoubtedly the *visco-resistive* regime: i.e., the response is both *linear* and *constant- $\psi$* .

According to Sec. IV F, the critical normalized error-field amplitude required to trigger a “downward” bifurcation of the plasma state is given by

$$\hat{\xi}_c = \begin{cases} P^{1/3} Q_0 R^{5/2} & \text{for } R \leq 1, \\ P^{1/3} Q_0 R^3 & \text{for } R > 1. \end{cases} \quad (146)$$

This critical value can be converted into the conventional measure of critical error-field strength,  $b_r/B_\phi$ , where  $b_r$  is the resonant radial component of the error-field *in vacuo* at the rational surface, via

$$\frac{b_r}{B_\phi} \approx \frac{r_s P^{1/6} S^{-1/3} \hat{\xi}_c}{R_0 q_s}. \quad (147)$$

Table I shows  $b_r/B_\phi$  calculated as a function of  $R_0$  for typical low-density, ohmically heated, target plasmas in JET-like tokamaks. It can be seen that the critical error-field amplitude is a *rapidly decreasing* function of increasing machine size. The predicted values of  $b_r/B_\phi$  for COMPASS-C, DIII-D, and JET-sized plasmas ( $3.2 \times 10^{-3}$ ,  $4.5 \times 10^{-4}$ , and  $1.3 \times 10^{-4}$ , respectively) lie within a factor of 2 of the experimental values found in these devices.<sup>27–29</sup> The critical error-field strength required to trigger a “downward” bifurcation in a reactor-sized plasma (i.e.,  $R_0 \sim 8$  m) is

$$\frac{b_r}{B_\phi} \sim 2 \times 10^{-5}, \quad (148)$$

indicating that reactor-sized tokamaks are likely to be hypersensitive to error-fields.

## VI. SUMMARY

The bifurcated states of a rotating tokamak plasma in the presence of a static, resonant, error-field are strongly analogous to the bifurcated states of a conventional induction motor. The two plasma states are the “unreconnected” state, in which the plasma rotates, generating strong “eddy currents”

at the rational surface which effectively suppress error-field-driven magnetic reconnection, and the “fully reconnected” state, in which the plasma rotation at the rational surface is arrested, the eddy currents are consequently weak, and driven magnetic reconnection proceeds without hindrance. Suppose that the plasma starts off in the “unreconnected” state. If the error-field amplitude is *very gradually* increased, a critical amplitude is eventually reached which triggers a bifurcation from the “unreconnected” to the “fully reconnected” state. This type of bifurcation, which is termed a “downward” bifurcation, is characterized by a sudden collapse in the plasma rotation interior to the rational surface, accompanied by the simultaneous formation of a “locked” (to the static error-field) magnetic island chain at the rational surface (with no rotating precursor). Of course, the formation of magnetic islands inside the plasma is associated with a degradation of the plasma confinement. If the error-field amplitude is now *very gradually* decreased, a critical amplitude is eventually reached which triggers a bifurcation from the “fully reconnected” to the “unreconnected” state. This type of bifurcation, which is termed an “upward” bifurcation, is characterized by a sudden recovery of the plasma rotation interior to the rational surface, accompanied by the simultaneous spin up and decay of the magnetic island chain at the rational surface. The decay of the magnetic islands inside the plasma is associated with an improvement in plasma confinement. The critical error-field amplitude needed to trigger a “downward” bifurcation is significantly *larger* than the critical amplitude needed to trigger an “upward” bifurcation. Thus, once locked magnetic islands have been introduced into a tokamak plasma, by means of an error-field, the error-field strength must be reduced significantly before they can be removed.

The response regime of a rotating plasma in the vicinity of the rational surface to a static, resonant, error-field is determined by *three* parameters: the normalized plasma viscosity,  $P$ , the normalized plasma rotation,  $Q_0$ , and the normalized plasma resistivity,  $R$ . These parameters are defined in Sec. III D. There are 11 distinguishable response regimes. The extents of these regimes in  $P$ – $Q_0$ – $R$  space are shown in Figs. 4 and 5. The critical error-field amplitude required to trigger a “downward” bifurcation in each of the 11 regimes is specified by Eqs. (124)–(134). There is effectively only one response regime associated with the “upward” bifurcation. The critical error-field amplitude required to trigger an “upward” bifurcation in this regime is specified by Eq. (140).

Error-field-driven magnetic reconnection can severely limit the available operating space for low-density, ohmically heated “target plasmas” in medium to large tokamaks.<sup>28,29</sup> This problem can be alleviated by reducing the amplitude of the resonant error-field. The appropriate response regime for a low-density, ohmically heated, target plasma is found to be the *Rutherford* regime for small tokamaks, and the *visco-resistive* regime for large tokamaks. The former regime is a nonlinear constant- $\psi$  regime, whereas the latter is a linear constant- $\psi$  regime. Note that, despite a previous report to the contrary,<sup>7</sup> it is legitimate to use the constant- $\psi$  approximation to describe the response of an

ohmic plasma to a static error-field. However, it is not legitimate to use this approximation to describe the response of a plasma subject to unbalanced NBI heating. The critical error-field amplitude required to induce a “downward” bifurcation in a low-density, ohmic target plasma is a strongly decreasing function of increasing machine size. The predicted critical amplitude in a reactor-sized plasma is extremely small (i.e.,  $b_r/B_\phi \sim 2 \times 10^{-5}$ ), indicating that particular care may need to be taken to eliminate resonant error-fields in reactors.

The analysis presented in this paper is essentially complete, within the restrictive framework of resistive, viscous MHD. In principle, the analysis could be generalized, in a fairly straightforward manner, using a more realistic treatment of the plasma which takes into account non-MHD effects, such as the finite ion Larmor radius, diamagnetic, and other drift, effects, electron inertia, the Hall effect, etc. The analysis could also be generalized to take into account the mode coupling due to toroidicity, finite plasma pressure, and plasma shaping. All of this is left to the future.

#### ACKNOWLEDGMENTS

The author is indebted to Dr. F. L. Waelbroeck (IFS) for many illuminating discussions during the preparation of this paper. This research was funded by the U.S. Department of Energy under Contract No. DE-FG05-96ER-54346.

<sup>1</sup>The conventional definition of this parameter is  $\beta = 2\mu_0 \langle p \rangle / \langle B^2 \rangle$ , where  $\langle \dots \rangle$  denotes a volume average,  $p$  is the plasma pressure, and  $B$  is the magnetic field-strength.

<sup>2</sup>The standard large-aspect-ratio, low- $\beta$  tokamak ordering is  $R_0/a \gg 1$  and  $\beta \sim (a/R_0)^2$ , where  $R_0$  and  $a$  are the major and minor radii of the plasma, respectively.

<sup>3</sup>Z. Chang and J. D. Callen, Nucl. Fusion **30**, 219 (1990).

<sup>4</sup>J. A. Wesson, R. D. Gill, M. Hugon, F. C. Schüller *et al.*, Nucl. Fusion **29**, 641 (1989).

- <sup>5</sup>R. Fitzpatrick, in *Theory of Fusion Plasmas*, Proceedings of the Joint Varenna-Lausanne International Workshop, Varenna 1992 (Società Italiana di Fisica, Bologna, 1992), p. 147.
- <sup>6</sup>R. Fitzpatrick, Nucl. Fusion **33**, 1049 (1993).
- <sup>7</sup>Z. W. Ma, X. Wang, and A. Bhattacharjee, Phys. Plasmas **3**, 2427 (1996).
- <sup>8</sup>X. Wang and A. Bhattacharjee, Phys. Plasmas **4**, 748 (1997).
- <sup>9</sup>O. A. Hurricane, T. H. Jensen, and A. B. Hassam, Phys. Plasmas **2**, 1976 (1995).
- <sup>10</sup>H. P. Furth, J. Killeen, and M. N. Rosenbluth, Phys. Fluids **6**, 459 (1963).
- <sup>11</sup>T. H. Stix, Phys. Fluids **16**, 1260 (1973).
- <sup>12</sup>The strong analogy between the bifurcation theory for error-field-driven reconnection in a rotating plasma and that for a conventional induction motor was pointed out to the author independently by C. G. Gimblett and M. K. Bevir of Culham Laboratory and T. H. Jensen of General Atomics.
- <sup>13</sup>R. Fitzpatrick, Phys. Plasmas **1**, 3308 (1994).
- <sup>14</sup>R. J. Hastie (private communication, 1992).
- <sup>15</sup>A. H. Boozer, Phys. Plasmas **3**, 4620 (1996).
- <sup>16</sup>P. H. Rutherford, Phys. Fluids **16**, 1903 (1973).
- <sup>17</sup>P. H. Rutherford, in *Basic Physical Processes of Toroidal Fusion Plasmas* Proceedings, Course and Workshop, Varenna, 1985 (Commission of the European Communities, Brussels, 1986), Vol. 2, p. 531.
- <sup>18</sup>F. L. Waelbroeck, Phys. Fluids B **1**, 2372 (1989).
- <sup>19</sup>F. L. Waelbroeck, Phys. Rev. Lett. **70**, 3259 (1993).
- <sup>20</sup>F. L. Waelbroeck, J. Plasma Phys. **50**, 477 (1993).
- <sup>21</sup>P. A. Sweet, *Electromagnetic Phenomena in Cosmical Physics* (Cambridge U.P., New York, 1958).
- <sup>22</sup>E. N. Parker, J. Geophys. Res. **62**, 509 (1957).
- <sup>23</sup>W. Park, D. A. Monticello, and R. B. White, Phys. Fluids **27**, 137 (1984).
- <sup>24</sup>K. Brau, M. Bitter, R. J. Goldston, D. Manos, K. McGuire, and S. Suckewer, Nucl. Fusion **23**, 1643 (1983).
- <sup>25</sup>D. Stork, A. Boileau, F. Bombarda *et al.*, in *Controlled Fusion and Plasma Physics 1987*, Proceedings of the 14th European Conference, Madrid (European Physical Society, Petit-Lancy, 1987), Vol. 1, p. 306.
- <sup>26</sup>J. Y. Chen, S. C. McCool, A. J. Wootton *et al.*, in *Research Using Small Tokamaks*, Proceeding of Technical Committee Meeting, Arlington 1990 (International Atomic Energy Authority, Vienna, 1990), p. 41.
- <sup>27</sup>T. C. Hender, R. Fitzpatrick, A. W. Morris *et al.*, Nucl. Fusion **32**, 2091 (1992).
- <sup>28</sup>J. T. Scoville, R. J. La Haye, A. G. Kellman, T. H. Osborne, R. D. Stambaugh, E. J. Strait, and T. S. Taylor, Nucl. Fusion **31**, 875 (1991).
- <sup>29</sup>G. M. Fishpool and P. S. Haynes, Nucl. Fusion **34**, 109 (1994).